Nanotechnology **18** (2007) 455606 (7pp) doi:10.1088/0957-4484/18/45/455606

An ionic liquid based synthesis method for uniform luminescent lanthanide fluoride nanoparticles

Nuria O Nuñez and Manuel Ocaña

Instituto de Ciencia de Materiales de Sevilla, CSIC, Americo Vespucio 49, 41092, Isla de la Cartuja, Sevilla, Spain

E-mail: mjurado@icmse.csic.es

Received 24 July 2007, in final form 6 September 2007
Published 10 October 2007
Online at stacks.iop.org/Nano/18/455606

Abstract
We describe a facile procedure for the synthesis of uniform lanthanide fluoride nanophosphors by homogeneous precipitation in ethylene glycol solutions containing lanthanide precursors and an ionic liquid (1-butyl, 2-methylimidazolium tetrafluoroborate). It is shown that the use of this ionic liquid as a fluoride source, an appropriate choice of the solvent and the lanthanide precursor, and the adjustment of reaction temperature, are essential to obtain uniform nanoparticles. This method is applied to the preparation of pure YF_3, EuF_3 and TbF_3 nanoparticles as well as of Eu-doped YF_3 and Tb-doped YF_3. In most cases, highly uniform nanoparticles were obtained, the size of which could be tuned in the nanometer range by adjusting the nature and concentration of the starting lanthanide precursor. The luminescent properties of the synthesized materials are also evaluated.

1. Introduction

Rare-earth (RE) based compounds attract much attention because of their luminescent properties which confer to them important applications in several fields of science and technology including optoelectronic (lasers [1], waveguide devices [2], etc) and biomedicine (biosensors and biological imaging) [3, 4], to mention a few. Many of these compounds consist of a crystalline host doped with a small amount of lanthanide (Ln) cations. Among the possible host matrices, lanthanide (Ln) fluorides are preferred because they have lower vibrational energies than oxides and consequently, the quenching of the exited state of the Ln cations is minimized, resulting in a higher quantum efficiency of the luminescence [5, 6].

Most of the above applications need uniform nanoparticles, which has led many scientists to develop procedures for the synthesis of such kind of particles. A large variety of approaches can be found in the literature for the synthesis of Ln-doped LaF_3 nanoparticles, which is perhaps the most studied system [3, 7–9]. However, much less attention has been paid to other fluoride hosts such as YF_3, which has been shown to be an interesting candidate for both up and down conversion phosphors [6, 10, 11]. To our knowledge, truly uniform Ln-doped YF_3 particles in the nanometer size range have not been yet obtained.

Ionic liquids (ILs) are non-volatile, non-flammable and thermally stable organic salts with low melting point, which have been recently suggested as a 'green' alternative to the conventional organic solvents for the synthesis of inorganic compounds [12, 13]. Among the main advantages of using ILs as solvents or additives in inorganic synthesis is their superior capability for the solvation and stabilization of metal cations, which gives to them the possibility of acting as capping agents or surfactants. These properties have been exploited to prepare nanoparticles of different composition (metals [14, 15], metal oxides [16], metal sulphides [17], etc). Very recently, it has been also shown that one of the most common IL (1-butyl,2-methylimidazolium tetrafluoroborate, $[BMIM]BF_4$) can be used for the synthesis of metal fluorides by precipitation when solutions of metal nitrates in this solvent are heated in a microwave oven [18]. The required fluoride anions were liberated by the IL as a consequence of its hydrolysis with the hydration water molecules of the metal precursors. It should be noted that although particles of different metal fluorides (Fe, Co, Zn, La, Y, Sr) with different morphologies were reported

in this work, they were rather heterogeneous in size and shape and/or strongly aggregated.

Herein, we describe a facile method for the synthesis of non-aggregated and highly uniform nanoparticles of YF_3 and Ln-doped YF_3 (Ln = red-emitting Eu(III) or green-emitting Tb(III) cations) [6], which involves the use of [BMIM]BF_4 as the fluoride source. It is shown that the key parameters to obtain uniform nanoparticles are the adjustment of the reaction temperature and an appropriate choice of the solvent and the Ln precursor. The procedure can be used for the synthesis of other LnF_3 nanoparticles, as illustrated for the case of pure EuF_3 and TbF_3. The luminescent properties of the synthesized materials are also evaluated.

2. Experimental details

2.1. Reagents

Yttrium (III) acetylacetonate ($Y(CH_3COCHCOCH_3)_3{\cdot}XH_2O$, Alpha, 99.9%), yttrium (III) acetate ($Y(CH_3COO)_3{\cdot}XH_2O$, Aldrich, 99.9%), yttrium (III) nitrate ($Y(NO_3)_3{\cdot}6H_2O$, Aldrich, 99.99%), europium (III) acetate hydrate ($Eu(CH_3COO)_3$, Alfa Aesar), europium (III) acetylacetonate ($Eu(CH_3COCHCOCH_3)_3{\cdot}3H_2O$, Alpha Aesar, 99.9%), europium (III) nitrate ($Eu(NO_3)_3{\cdot}5H_2O$, Aldrich, 99.9%), terbium (III) acetylacetonate ($Tb(CH_3COCHCOCH_3)_3$, Alpha Aesar, 99.9%) and terbium nitrate hydrate ($Tb(NO_3)_3$, Alfa Aesar, 99.9%) were selected as Ln precursors. 1-Butyl, 2-methylimidazolium tetrafluoroborate, ($C_8H_{15}BF_4N_2$, Fluka, >97%) and ammonium fluoride (NH_4F, Aldrich, >99%) were used as fluoride sources and ethylene glycol (Fluka, <99.5%) and ethanol (Panreac, absolute), as solvents. All chemicals were used as received.

2.2. Nanoparticle synthesis

The standard procedure for the synthesis of the rare-earth fluoride nanoparticles was as follows. Weighed amounts of the rare-earth precursors were dissolved in ethylene glycol under magnetic stirring, heating the vial at ∼100 °C to facilitate the dissolution process. When using ethanol as solvent, the dissolution of the Ln precursors was carried out at room temperature. The ethylene glycol solutions were cooled down to room temperature, after which the desired volume of [BMIM]BF_4 was admixed while keeping the magnetic stirring. The final solutions (total volume = 10 cm^3) were then aged for 15 h in tightly closed test tubes using an oven preheated at the selected temperature. After aging, the resulting dispersions were cooled down to room temperature, centrifuged to remove the supernatants and washed, twice with ethanol and once with double distilled water. For some analyses, the powders were dried at room temperature.

2.3. Characterization

The shape of the nanoparticles was examined by transmission electron microscopy (TEM, Philips 200CM). For this, a droplet of an aqueous suspension of the samples was deposited on a copper grid coated with a transparent polymer and dried. The particle size distributions were obtained from the micrographs by counting several hundreds of particles.

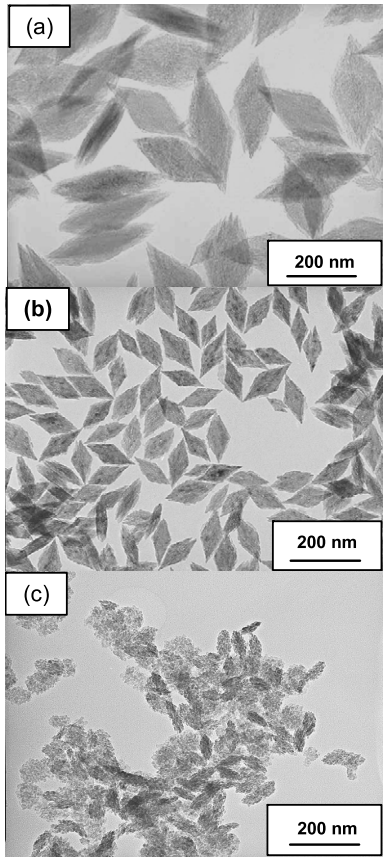

Figure 1. TEM images of the particles obtained from $Y(acac)_3$ (a), $Y(OAc)_3$ (b) and $Y(NO_3)_3$ (c) under the conditions described in the text.

To obtain structural information on the prepared nanoparticles, we used x-ray diffraction (Siemens D501) and high-resolution transmission electron microscopy (HRTEM, Philips 200CM). The digital diffraction patterns were obtained from the HRTEM images by using digital micrograph software.

The qualitative composition of the precipitated particles was assessed by energy dispersive x-ray analysis (EDX, Philips DX4) coupled to the TEM microscope. The excitation and emission spectra of the samples dispersed in water were measured in a Horiba Jobin-Yvon spectrofluorimeter (Fluorolog fl3-11) operating with a slit of 1.5 nm.

3. Results and discussion

In order to establish the optimum conditions for the formation of luminescent RE fluoride nanoparticles, we first addressed the synthesis of pure YF_3. The effects of reaction temperature, Y(III) concentration and IL/Y(III) ratio on the morphological characteristics of the particles were studied using yttrium(III) acetylacetonate ($Y(acac)_3$) as the Y source and ethylene glycol as solvent. It was observed that the aging temperature was a critical factor for the formation of uniform dispersions. Thus, for 0.02 mol dm^{-3} solutions of this precursor and 6.7 mol dm^{-3} of IL, uniform particles with rhombic shape (figure 1(a)) and longer and shorter diagonals of 230 and 85 nm, respectively (table 1), were obtained if the aging

Table 1. Size of the particles synthesized from ethylene glycol solutions of different Ln precursors at constant IL concentration (6.7 mol dm^{-3}) and aging temperature (120 °C). The standard deviations are shown in parentheses.

Y(III) precursor	Eu(III) precursor	Tb(III) precursor	[Y(III)] (mol dm^{-3})	[Eu(III)] (mol dm^{-3})	[Tb(III)] (mol dm^{-3})	Particle size by TEM		
						Long axis (nm)	Short axis (nm)	Thickness (nm)
$Y(acac)_3$	—	—	0.005	—	—	340 (35)	178 (25)	70 (9)
$Y(acac)_3$	—	—	0.02	—	—	230 (29)	85 (10)	50 (7)
$Y(acac)_3$	—	—	0.1	—	—	240 (25)	110 (20)	34 (5)
YAc_3	—	—	0.02	—	—	130 (13)	54 (8)	23 (3)
YAc_3	$Eu(NO_3)_3$	—	0.02	0.002	—	110 (10)	38 (3)	26 (1)
YAc_3	—	$Tb(NO_3)_3$	0.02	—	0.002	110 (10)	44 (6)	26 (3)
—	$Eu(acac)_3$	—	—	0.02	—	12 (1)	6 (0.8)	—
—	—	$Tb(acac)_3$	—	—	0.02	60 (6)	17 (4)	14 (3)

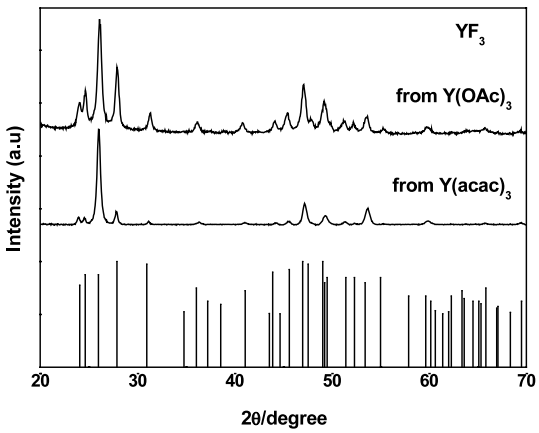

Figure 2. X-ray diffraction patterns of the particles obtained from $Y(acac)_3$ and $Y(OAc)_3$. The reference pattern for orthorhombic YF_3 obtained from the JCPDS file is also included.

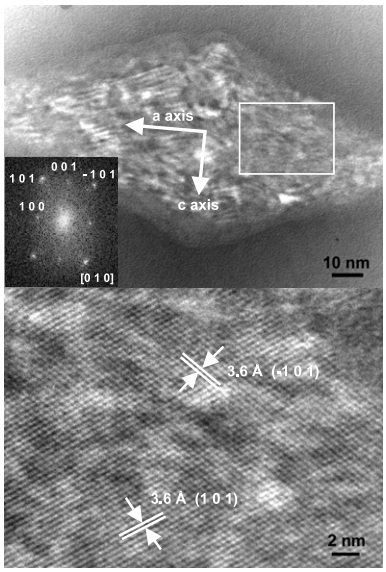

Figure 3. Upper: HRTEM image of a single YF_3 nanoparticle; the inset shows the digital electron diffraction pattern obtained from the HRTEM image. Lower: magnification of the rectangular zone marked in the figure for a better observation of the crystallographic planes.

temperature was 120 °C. These particles were identified by x-ray diffraction (XRD, figure 2) as orthorhombic YF_3.[1] The fluoride anions required for the precipitation of this phase are provided by the BF_4^- anions of the IL, which, as has been previously suggested [18], undergo fast hydrolysis with the hydration water molecules coming from transition metal salts ($Y(acac)_3$, in our case) on heating according to the reaction

$$BF_4^-(\mathrm{IL}) + H_2O \rightarrow BF_3{\cdot}H_2O(\mathrm{IL}) + F^-(\mathrm{IL}).$$

However, at <100 °C, no precipitation was detected, suggesting that no appreciable hydrolysis of $[BMIM]BF_4$ took place at this temperature, whereas an increase of the reaction temperature up to 200 °C resulted in strongly agglomerated and smaller (20 nm) nanoparticles.

A detailed observation of figure 1(a) suggests that the particles were flat, and some of them lay with the rhombic faces perpendicular to the TEM grid plane, from which a particle thickness of 50 nm (table 1) was roughly estimated. This morphology would explain the differences in the relative intensity of the XRD reflections detected between our sample and the JCPDF file (figure 2), as a consequence of a preferential orientation of the particles with the rhombus faces parallel to the sample holder. From the enhancement of the reflections corresponding to the (0*k*0) planes, it could be assumed that the crystallographic *b*-axis of the particles was perpendicular to the rhombic faces. These suggestions were confirmed by HRTEM microscopy and the digital diffraction patterns (DDPs) obtained from the HRTEM image of a single particle lying on its rhombic face (figure 3). Thus, the whole set of spots observed in the DDP corresponds to the [010] zone axis of orthorhombic YF_3[Note 1], indicating that the crystallographic *b*-axis was perpendicular to the rhombus facets. Furthermore, some of these spots could be assigned to the (100) and (001) planes of such phase, the first one being aligned normally to the longest particle dimension, which manifests that the *a*-axis was parallel to the longest rhombus diagonal and therefore that the *c*-axis was parallel to the shorter one. The (101) and ($\bar{1}$01) planes could also be clearly observed in the magnified zone of the HRTEM image shown in the lower part of the figure.

It was also found that a decrease of the IL concentration from 6.7 to 3.35 mol dm^{-3} did not have a noticeable influence on particle size and shape, but the increase of this concentration to 13.4 mol dm^{-3} resulted in strongly aggregated tiny entities. Therefore, it seems that the formation of uniform particles in

[1] JCPDS file no. 32-1431.

this system requires a precise reaction rate. If precipitation takes place too quickly, either by increasing the temperature up to 200 °C or the IL concentration (and therefore, the amount of fluoride anions), heterogeneous dispersions are obtained.

As observed in table 1, the decrease of the Y(III) concentration from 0.02 to 0.005 mol dm^{-3} resulted in an increase of particle size (340 nm × 178 nm × 70 nm), which could be explained with the classical theory of solution nucleation and particle growth [19]. Thus, as the Y(III) concentration decreases, the precipitation reaction should become slower, decreasing the number of nuclei which further grow to a higher size. An increase of the Y(III) concentration from 0.02 to 0.1 mol dm^{-3} did not give rise to significant changes in particle size (table 1). However, an important reduction of particle dimensions (130 nm × 54 nm × 23 nm) (table 1) without changes in morphology (figure 1(b)) or crystalline structure (figure 2) did result when $Y(acac)_3$ was replaced by yttrium acetate ($Y(OAc)_3$) keeping constant the other experimental conditions used to prepare the particles shown in figure 1(a). The use of other Y(III) sources such as Y(III) nitrate yielded ill-defined particles with smaller sizes (figure 1(c)). These results manifest the strong influence of the Y(III) precursor on the morphological characteristics of the precipitated particles, which has been also previously observed for the formation of other inorganic compounds in polyol medium [20]. It must be mentioned that the use of ethylene glycol as solvent is also a critical factor for the formation of uniform particles, since the change of ethylene glycol to ethanol keeping the other experimental conditions within the range required for the formation of uniform dispersions gave rise to ill-defined gel-like precipitates. The role played by polyols in the synthesis of microparticles and nanoparticles of several inorganic compounds, including RE-doped CeF_3 [21] and LaF_3 [22], has been well documented and mainly ascribed to the reducing, cation complexing and surface protection abilities of these solvents [20].

It is also important to mention that the presence of $[BMIM]BF_4$ is essential to obtain uniform particles through the procedure reported here, since the change of IL to another fluoride source such as NH_4F always gave rise to strongly agglomerated and almost equiaxed particles (<100 nm) of an unidentified crystalline compound (data not shown). This finding indicates that, in our synthesis procedure, $[BMIM]BF_4$ acts not only as a fluoride supplier but also as a morphology-directing agent.

Therefore, it can be concluded that by using the method reported here, the size of the YF_3 particles can be tuned between 340 and 130 nm (longest particle dimension) by varying the yttrium precursor concentration or by changing the yttrium precursor nature. It should be noted that a few works can be found in the literature that report procedures for the preparation of uniform YF_3 particles with ellipsoidal shape (length ∼300 nm) [23, 24] and other morphologies (∼100 nm) [25], involving in all cases a highly toxic fluoride source (NH_4HF_2) and solvents (cyclohexane, octadecylamine) in the synthesis processes.

For the doping experiments, we selected $Y(OAc_3)$ as the yttrium precursor since, as described above, this salt yielded the smallest uniform particles. It was found that the addition of $Eu(NO_3)_3$ (Eu/Y atomic ratio = 0.1) or $Tb(NO_3)_3$ (Tb/Y atomic ratio = 0.1) to the starting solution had no effect on particle morphology (figure 4), although a decrease in particle size (110 nm × 38 nm × 26 nm, for the Eu-doped sample and 110 nm × 44 nm × 26 nm, for the Tb-doped one) with respect to the undoped system was detected (table 1). The XRD patterns of the doped samples only displayed the reflections corresponding to orthorhombic YF_3 (data not shown), which might be an indication of the success of the doping procedure. The incorporation of Eu(III) or Tb(III) cations in the YF_3 matrix was corroborated by EDX analyses since the spectra obtained for several single particles were always very similar, showing the Eu or Tb peaks in addition to those of yttrium (figure 5).

In order to investigate the applicability of the procedure reported here to other lanthanide fluorides, the synthesis of pure europium and terbium fluorides was also addressed under similar experimental conditions to those involved in

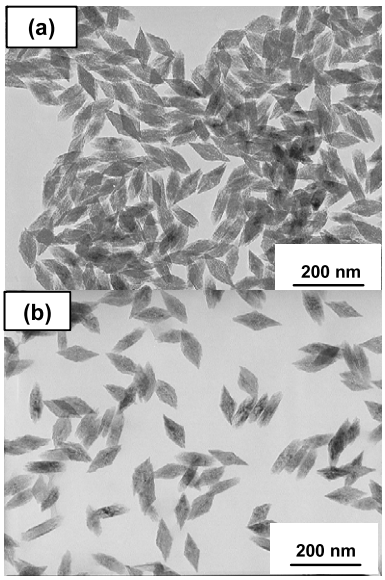

Figure 4. TEM images of the Eu^{3+}-doped YF_3 (a) and Tb^{3+}-doped YF_3 (b) nanoparticles prepared as described in table 1.

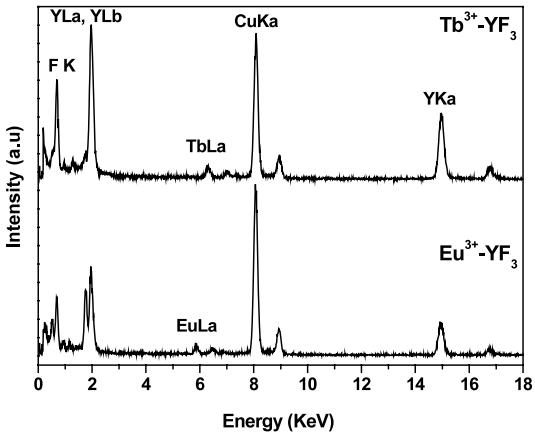

Figure 5. EDX spectra of the Eu^{3+}-doped YF_3 and Tb^{3+}-doped YF_3 nanoparticles shown in figures 4(a) and (b). The most intense peak for each element has been labeled.

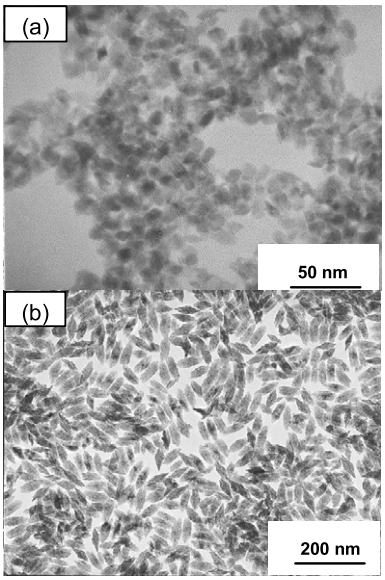

Figure 6. TEM images of the europium fluoride (a) and terbium fluoride (b) nanoparticles prepared as described in table 1.

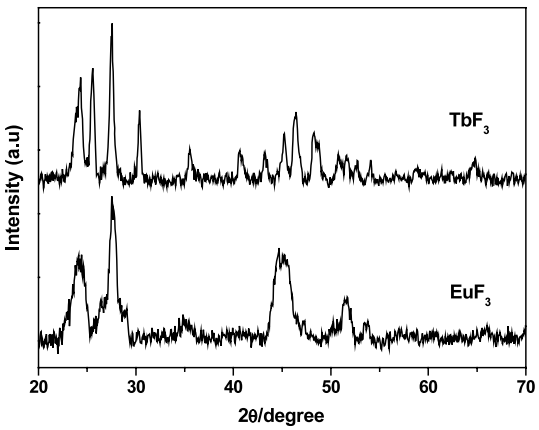

Figure 7. X-ray diffraction patterns of the EuF_3 and TbF_3 nanoparticles shown in figures 6(a) and (b), respectively.

the synthesis of the rhombic YF_3 plates shown in figure 1(b) but using europium or terbium acetylacetonates as precursors. As observed in figure 6, whereas for the terbium system nanoparticles with the same morphology as those observed for YF_3 (figure 1(b)) but with smaller size (60 nm × 17 nm × 14 nm) (table 1) were obtained, much smaller particles (12 nm × 6 nm) (table 1) with ovoidal shape resulted in the europium case. It is important to mention that according to XRD (figure 7), the TbF_3 nanoparticles crystallized in the orthorhombic phase[2] as in the case of YF_3, whereas the EuF_3 did in the hexagonal one[3]. These results are in agreement with a previous report by Wang *et al* [24], who synthesized pure lanthanide fluorides from water/ethanol solutions of Ln salts and NH_4HF_2, which were hydrothermally treated in the presence of linoleic acid and sodium linoleate added as surface protecting agents. They also found that elongated particles (∼300 nm) only resulted

[2] JCPDS file no. 37-1487.
[3] JCPDS file no. 32-0373.

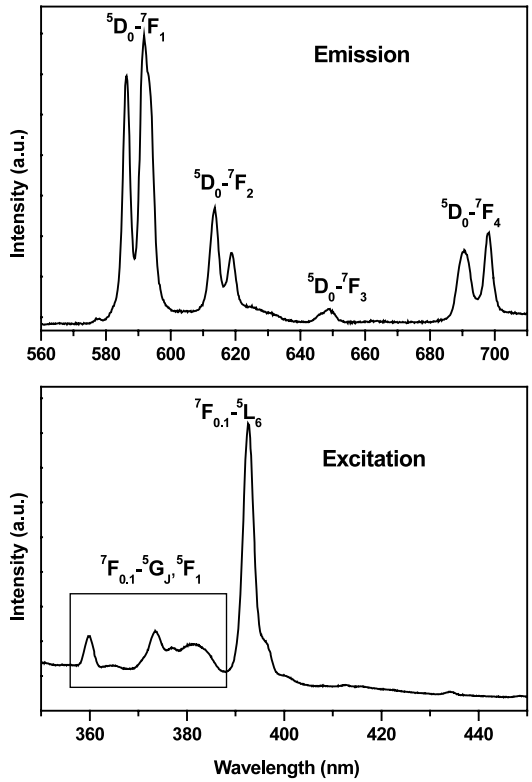

Figure 8. Emission ($\lambda_{ex} = 392$ nm) and excitation ($\lambda_{em} = 593$ nm) spectra of the Eu^{3+}-doped YF_3 nanoparticles.

for orthorhombic fluorides (as the YF_3 case), whereas nearly round particles were formed for the systems crystallizing in the hexagonal phase (from La to Nd). These morphological differences were attributed by these authors to the different crystallization behavior of each kind of particle. Incidentally, in the above report no information on particle size and shape is given for the TbF_3 system, whereas it is stated that the procedure failed for the EuF_3 case.

The excitation (monitored through the emission at 593 nm) and emission (excitation at 392 nm) spectra recorded for the Eu-doped YF_3 nanoparticles illustrated in figure 4(a) are shown in figure 8. Both spectra are in accordance with those previously reported for this system [6, 10, 11], displaying excitation bands in the 350–400 nm region with the most intense one at 393 nm, corresponding to the f–f electronic transitions characteristics of the Eu^{3+} ions [6] and several fluorescence bands between 560 and 720 nm whose assignment [6] is given in the figure. As observed, all luminescence bands were very sharp (width at half maxima 3–4 nm) and the most intense ones appeared at 585 and 591 nm, causing a strong red luminescence for this material. The excitation (monitored at 593 nm) and emission (excitation at 392 nm) spectra recorded for the pure EuF_3 nanoparticles (figure 9) were similar to those previously reported [26, 27], and at the same time to those corresponding to the Eu-doped YF_3 sample (figure 8). This is not surprising, since the energy of the Eu^{3+} levels is hardly affected by the crystal field due to the shielding effect of the $5s^25p^6$ electrons. The most remarkable difference between the emission spectra of both systems is that the bands of the pure EuF_3 nanoparticles were

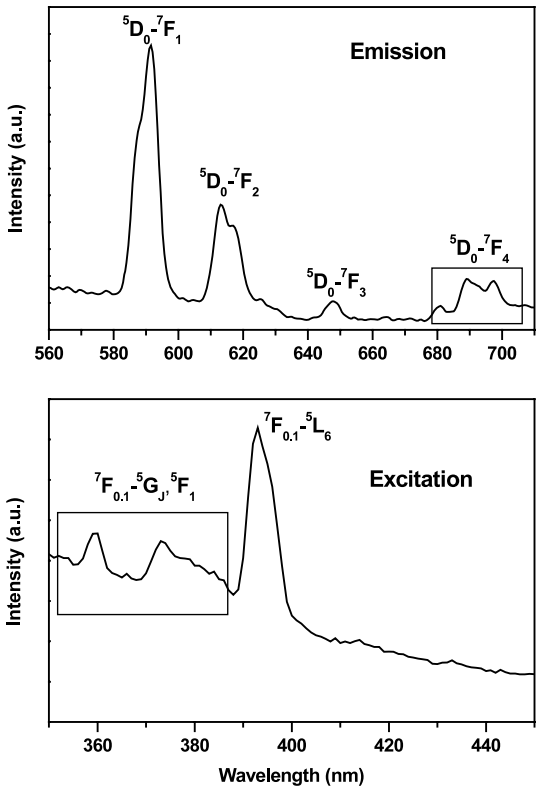

Figure 9. Emission ($\lambda_{ex} = 392$ nm) and excitation ($\lambda_{em} = 593$ nm) spectra of the EuF_3 nanoparticles.

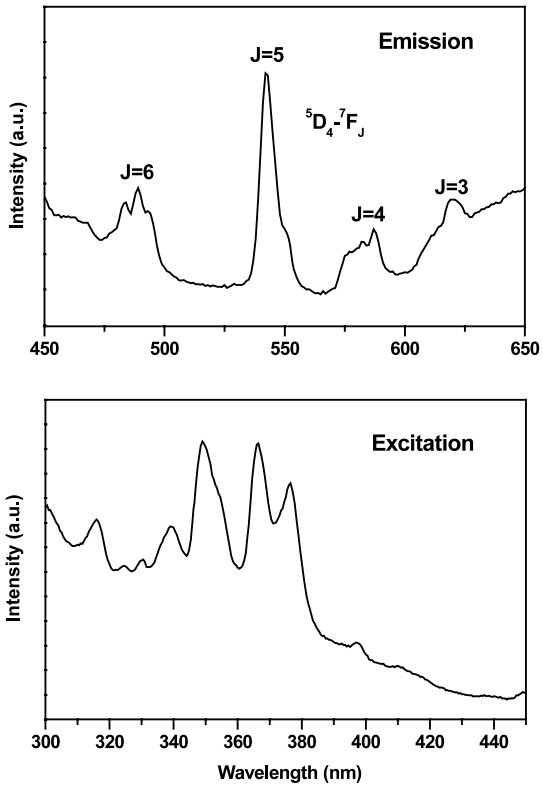

Figure 10. Emission ($\lambda_{ex} = 349$ nm) and excitation ($\lambda_{em} = 543$ nm) spectra of the Tb^{3+}-doped YF_3 nanoparticles.

broader than those of the Eu-doped sample; some of them even appeared overlapped. This behavior could be attributed to the smaller size of the particles of the former sample (table 1) following a previous report by Williams *et al* [28] on Eu-doped Y_2O_3, according to which the emission bands became broader as particle size decreased due to the disorder induced as the surface area of the nanocrystals increased.

Finally, the excitation (monitored at 543 nm) and emission (excitation at 349 nm) spectra obtained for the Tb-doped YF_3 and TbF_3 nanoparticles are shown in figures 10 and 11 respectively. As for the studied europium systems, the excitation spectra were similar for both samples, displaying several excitation bands in the 300–450 nm region, the most intense ones appearing at 349 and 366 nm, which was in agreement with a previous report on Tb-doped CaF_2 [29]. As expected, when excited at 349 nm, a green emission resulted for both terbium systems associated to the dominant emission band observed at 543 nm, which along with the other weaker bands in the 450–650 nm region (figure 11) arise from the $^5D_4$–^7F_j ($j = 1, 2, 3, 4$) transitions typical of the Tb(III) cations [4, 6, 29].

4. Conclusions

A facile procedure for the synthesis of uniform lanthanide fluoride nanoparticles by precipitation in ethylene glycol solutions containing lanthanide precursors and an ionic liquid (1-butyl,2-methylimidazolium tetrafluoroborate) as fluoride anion source has been developed. Here, we illustrate the

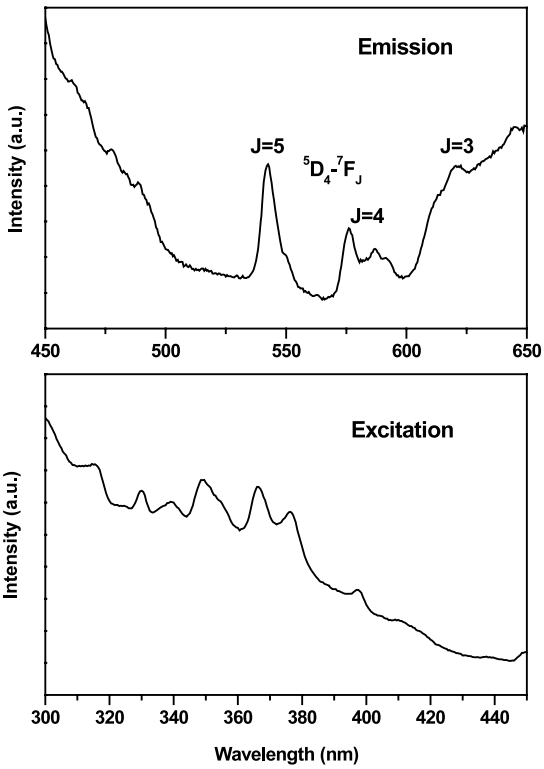

Figure 11. Emission ($\lambda_{ex} = 349$ nm) and excitation ($\lambda_{em} = 543$ nm) spectra of the TbF_3 nanoparticles.

preparation of pure YF_3, EuF_3 and TbF_3 as well as of Eu-doped and Tb-doped YF_3 nanoparticles, although this method

could be easily extended to other lanthanide fluoride systems with different applications. In the cases of pure terbium fluoride and the doped systems, highly uniform nanoparticles with orthorhombic structure and rhombic shape were obtained, the size of which could be tuned in the nanometer range by adjusting the nature and concentration of the starting lanthanide precursor. However, less homogeneous hexagonal phase EuF_3 nanoparticles with ellipsoidal shape were obtained, which was attributed to the different crystalline structure resulting in this case. The samples containing europium(III) showed a strong red emission, whereas a green emission was detected for those containing terbium(III), which are characteristics of these lanthanide cations.

Acknowledgments

This work has been funded by the Ramón Areces Foundation and by the Spanish Ministerio de Educación y Ciencia under grants ENE2004-01657 and MAT2005-03028. N O Nuñez wants to thank the Spanish Ministerio de Educación y Ciencia for a Juan de la Cierva contract. We also acknowledge Dr A Barranco, Dr C López-Cartes and Dr C Rojas for their technical assistance in the characterization of the samples by fluorescence spectroscopy and HRTEM, respectively.

References

[1] Huber G, Heumann E, Sandrock T and Petermann K 1997 *J. Lumin.* **72–74** 1
[2] Dekker R, Klunder D J W, Borreman A, Diemeer M B J, Wörhoff K, Driessen A, Stouwdam J W and van Veggel F C J M 2004 *Appl. Phys. Lett.* **85** 6104
[3] Wang F, Zhang Y, Fan X and Wang M 2006 *Nanotechnology* **17** 1527
[4] Kong D I, Wang Z L, Lin C K, Quan Z W, Li Y Y, Li C X and Lin J 2007 *Nanotechnology* **18** 075601
[5] Stouwdam J W and van Veggel F C J M 2002 *Nano Lett.* **2** 733
[6] Yan R and Li Y 2005 *Adv. Funct. Mater.* **15** 763
[7] De G, Qin W, Zhang J, Zhao D and Zhang J 2005 *Chem. Lett.* **34** 914
[8] Yi G and Chow G 2005 *J. Mater. Chem.* **15** 4460
[9] Wang F, Zhang Y, Fan X and Wang M 2006 *J. Mater. Chem.* **16** 1031
[10] Cui Y, Fan X, Hong Z and Wang M 2006 *J. Nanosci. Nanotechnol.* **6** 830
[11] Tao F, Wang Z, Yao L, Cai W and Li X 2007 *J. Phys. Chem.* **111** 3241
[12] Antonietti M, Kuang D, Smarsly B and Zhou Y 2004 *Angew. Chem. Int. Edn* **43** 4988
[13] Klingshirn M A, Spear S K, Holbrey J D and Rogers R D 2005 *J. Mater. Chem.* **15** 5174
[14] Kim K, Choi S, Cha J, Yeon S and Lee H 2006 *J. Mater. Chem.* **16** 1315
[15] Wang Y and Yang H 2005 *J. Am. Chem. Soc.* **127** 5316
[16] Nakashima T and Kimizuka N 2003 *J. Am. Chem. Soc.* **125** 6386
[17] Jiang Y and Zhu Y 2004 *Chem. Lett.* **33** 1390
[18] Jacob D S, Bitton L, Grinblat J, Felner I, Koltypin Y and Gedanken A 2006 *Chem. Mater.* **18** 3162
[19] Lamer V K and Dinegar R J 1950 *J. Am. Chem. Soc.*. **72** 4847
[20] Poul L, Ammar S, Jouini N and Fievet F 2003 *J. Sol–Gel Sci. Technol.* **26** 261
[21] Wang Z L, Quan Z W, Jia P Y, Lin C K, Luo Y, Chen Y, Fang J, Zhou W, O'Connor C J and Lin J 2006 *Chem. Mater.* **18** 2030
[22] Wei Y, Lu F, Zhang X and Chen D 2007 *Mater. Lett.* **61** 1337
[23] Wang X, Zhuang J, Peng Q and Li Y 2005 *Nature* **437/1** 121
[24] Wang X, Zhuang J, Peng Q and Li Y 2006 *Inorg. Chem.* **45** 6661
[25] Lemyre J L and Ritcey A M 2005 *Chem. Mater.* **17** 3040
[26] Wang M, Huang Q L, Hong J M, Chen X T and Xue Z L 2006 *Cryst. Growth Des.* **6** 1972
[27] Zhuravleva N G, Sapoletova N A, Eliseev A A, Lukashin A V, Tretyakov Y D and Kynast U 2006 *Opt. Mater.* **28** 606
[28] Williams D K, Yuan H and Tissue B M 1999 *J. Lumin.* **83/84** 297
[29] Godbole S V, Nagpal J S and Page A G 2000 *Radiat. Meas.* **32** 343